ORGANIC LETTERS

2011
Vol. 13, No. 20
5424–5427

Organic Dyes Incorporating the Benzo[1,2-*b*:4,5-*b*′]dithiophene Moiety for Efficient Dye-Sensitized Solar Cells

Xiaoli Hao, Mao Liang,* Xiaobing Cheng, Xiaoqing Pian, Zhe Sun, and Song Xue*

Department of Applied Chemistry, Tianjin University of Technology, Tianjin 300384, People's Republic of China

liangmao717@126.com; xuesong@ustc.edu.cn

Received July 11, 2011

ABSTRACT

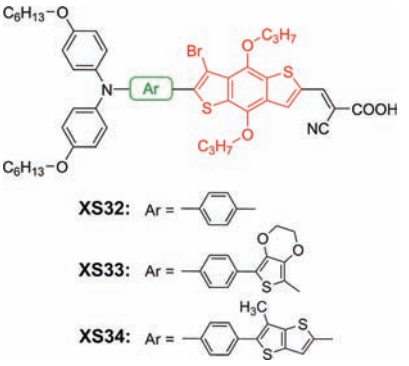

A new class of organic sensitizers incorporating a benzo[1,2-*b*:4,5-*b*′]dithiophene (BDT) unit as conjugated spacer has been synthesized and successfully used for dye-sensitized solar cells (DSSCs). The length of the π-conjugated spacers has a strong impact on electro-optical properties of these dyes, leading to the conversion efficiencies ranging from 4.17 to 5.68% under AM 1.5 G irradiation. This result indicates that the BDT unit is a promising candidate in organic sensitizers.

There has been considerable interest to develop cheap and easily accessible renewable energy sources due to increasing energy demands and concerns about global warming. Compared to traditional silicon-based solar cells, dye-sensitized solar cells (DSSCs) are viewed as promising candidates for renewable clean energy sources by virtue of their low manufacturing cost and impressive photovoltaic performance.[1] To achieve high solar power conversion efficiency, great research efforts are focused on designing and synthesizing new photosensitizers: Ru-based complexes[2] and organic sensitizers.[3,4] The former holds the record of validated efficiency of over 11%.[2c] Organic sensitizers with robust availability, ease of structural tuning, and generally high molar extinction coefficients, have emerged as a competitive alternative to the Ru-based counterpart.[5] So far, the metal-free organic sensitizers have gained promising solar energy-to-electricity conversion efficiencies (η) comparable to Ru-based complexes.[6]

(1) (a) O'Regan, B. C.; Grätzel, M. *Nature* **1991**, *353*, 737. (b) Grätzel, M. *Nature* **2001**, *414*, 338.

(2) (a) Chiba, Y.; Islam, A.; Watanabe, Y.; Komiya, R.; Koide, N.; Han, L. *Jpn. J. Appl. Phys.* **2006**, *45*, 24. (b) Gao, F.; Wang., Y.; Shi, D.; Zhang, J.; Wang, M.; Jing, X.; Humphry-Baker, R.; Wang, P.; Zakeeruddin, S. M.; Grätzel, M. *J. Am. Chem. Soc.* **2008**, *130*, 10720. (c) Nazeeruddin, M. K.; DeAngelis, F.; Fantacci, S.; Selloni, A.; Viscardi, G.; Liska, P.; Ito, S.; Takeru, B.; Grätzel, M. *J. Am. Chem. Soc.* **2005**, *127*, 16835.

(3) Hagfeldt, A.; Boschloo, G.; Sun, L.; Kloo, L.; Pettersson, H. *Chem. Rev.* **2010**, *110*, 6595 and references cited therein.

(4) (a) Liang, Y.; Peng, B.; Liang, J.; Tao, Z.; Chen, J. *Org. Lett.* **2010**, *12*, 1204. (b) Li, J.; Chen, C.; Lee, C.; Chen, S.; Lin, T.; Tsai, H.; Ho, K.; Wu, C. *Org. Lett.* **2010**, *12*, 5454. (c) Yang, H.; Yen, Y.; Hsu, Y.; Chou, H.; Lin, J. *Org. Lett.* **2010**, *12*, 16. (d) Cao, D.; Peng, J.; Hong, Y.; Fang, X.; Wang, L.; Meier, H. *Org. Lett.* **2011**, *13*, 1610. (e) Kumar, D.; Thomas, K.; Lee, C.; Ho, K. *Org. Lett.* **2011**, *13*, 2622. (f) Kwon, T.; Armel, V.; Nattestad, A.; MacFarlane, D.; Bach, U.; Lind, S.; Gordon, K.; Tang, W.; Jones, D.; Holmes, A. *J. Org. Chem.* **2011**, *76*, 4088. (g) Paek, S.; Choi, H.; Choi, H.; Lee, C.; Kang, M.; Song, K.; Nazeeruddin, M.; Ko, J. *J. Phys. Chem. C* **2010**, *114*, 14646.

(5) Mishra, A.; Fischer, M. K. R.; Bäuerle, P. *Angew. Chem., Int. Ed.* **2009**, *28*, 2474.

(6) (a) Ito, S.; Miura, H.; Uchida, S.; Takata, M.; Sumioka, K.; Liska, P.; Comte, P.; Péchy, P.; Grätzel, M. *Chem. Commun.* **2008**, 5194. (b) Zeng, W.; Cao, Y.; Bai, Y.; Wang, Y.; Shi, Y.; Zhang, M.; Wang, F.; Pan, Y.; Wang, P. *Chem. Mater.* **2010**, *22*, 1915. (c) Im, H.; Kim, S.; Park, C.; Jang, S.; Kim, C.; Kim, K.; Park, N.; Kim, C. *Chem. Commun.* **2010**, 1335.

10.1021/ol201858b
Published on Web 09/29/2011

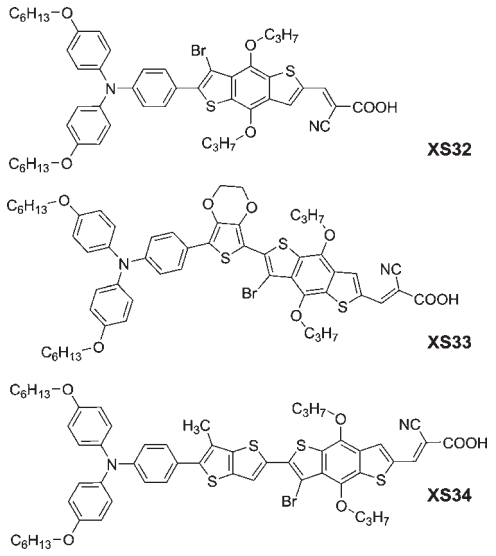

Figure 1. Structure of dyes.

Aside from electron donor (D) and acceptor (A) in a typical D−π−A system, the conjugated bridging segment (π) is widely recognized for its significance for performance control of DSSCs. Introduction of fused ring building blocks,[7,6b] involving cyclopentadithiophene, thieno[3,4-*b*]-thiophene, and dihexyl-substituted dithienosilole in the π-spacer, has proved to be an effective strategy for enhancing the light-harvesting capacity, leading to impressive performances under standard global air mass 1.5 (AM 1.5 G) illumination. Development of new fused ring building blocks may lead to synthesis of interesting photosenzitizers with tailor-made photophysical, electrochemical, and other properties to fulfill those requirements for high performance of DSSCs.

Recently, copolymers containing benzo[1,2-*b*:4,5-*b*′]-dithiophene (BDT) as the donor unit have exhibited outstanding photovoltaic properties for applications in polymer bulk heterojunction (BHJ) solar cells.[8] There are two merits of choosing BDT as the π-conjugated spacer of organic dyes for DSSCs: First, the large planar conjugated structure favors light harvesting and thermal stability. Second, higher oxidation potential of BDT relative to fused thiophene (e.g., thieno[3,4-b]thiophene) may result in high open-circuit voltage.[9] Thus, the BDT unit can be an attractive component in organic sensitizers. However, organic dyes based on a BDT unit have not been reported to our best knowledge. We therefore set out to synthesize compounds consisting of a BDT unit for constructing wide-spectral response organic chromophores for DSSCs (**XS32**−**34**, Figure 1).

Scheme 1. Synthetic Route of Dyes

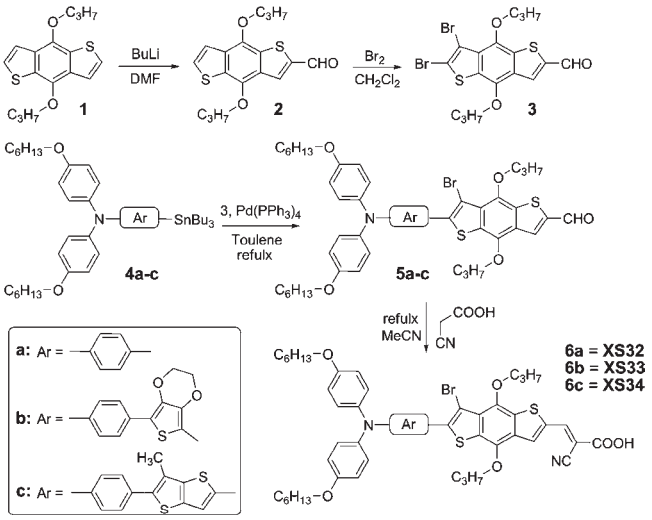

In order to investigate the structural modification of the spacer group upon the photophysical, electrochemical, and photocurrent action spectra and current−voltage characteristics of the DSSCs, single and binary π-conjugated spacers were applied into these dyes, apart from the blocks of a lipophilic alkoxy-substituted triphenylamine electron donor (D) and a hydrophilic cyanoacrylic acid electron acceptor (A). The synthetic route of **XS32**−**34** is shown in Scheme 1. The propoxy-substituted BDT moiety was synthesized and purified according to the literature.[8a] Treatment of the intermediate **1** with n-BuLi and DMF afforded aldyhyde **2**. Intermediate **3** was prepared from bromonation reaction with bromine. Reaction of **3** with **4a**−**c** via the palladium-catalyzed Stille coupling reaction afforded aldyhydes **5a**−**c**, which underwent Knoevenagel condensation with cyanoacetic acid to form the target dyes. These compounds are soluble in common organic solvents.

The optical and electrochemical properties of the three dyes are summarized in Table 1. In CH_2Cl_2 solution (Figure 2), the dyes display uninterrupted strong absorption between 350−550 nm, which is desirable for harvesting more solar light. The dyes **XS33** and **XS34** featuring a BDT-based binary spacer have a maximum molar absorption coefficient (ε) of 39×10^3 M^{-1} cm^{-1} at 483 and 502 nm, respectively. While the maximum molar absorption coefficient of **XS32** is reduced to 22×10^3 M^{-1} cm^{-1} at 472 nm. This observation could be rationalized in terms of an obviously electron-richer character of the binary spacer. Upon adsorption onto TiO_2, **XS33**−**34** show similar hypsochromic effect compared with that measured in solution [Figure S2a, Supporting Information (SI)], which could be ascribed to a weaker electron-withdrawing capability of the carboxylate titanium assembly than the carboxylic acid.[10]

(7) (a) Chen, D.; Hsu, Y.; Hsu, H.; Chen, B.; Lee, Y.; Fu, H.; Chung, M.; Liu, S.; Chen, H.; Chou, P. *Chem. Commun.* **2010**, 5256. (b) Zhang, G. L.; Bala, H.; Cheng, Y. M.; Shi, D.; Lv, X. J.; Yu, Q. J.; Wang, P. *Chem. Commun.* **2009**, 2198. (c) Paek, S.; Choi, H.; Choi, H.; Lee, C.; Kang, M.; Song, K.; Nazeeruddin, M. K.; Ko, J. *J. Phys. Chem. C* **2010**, *114*, 14646. (d) Qin, H.; Wenger, S.; Xu, M.; Gao, F.; Jing, X.; Wang, P.; Zakeeruddin, S. M.; Grätzel, M. *J. Am. Chem. Soc.* **2008**, *130*, 9202.

(8) (a) Liang, Y.; Wu, Y.; Feng, D.; Tsai, S.; Son, H.; Li, G.; Yu, L. *J. Am. Chem. Soc.* **2009**, *131*, 56. (b) Liang, Y.; Feng, D.; Wu, Y.; Tsai, S.; Li, G.; Ray, C.; Yu, L. *J. Am. Chem. Soc.* **2009**, *131*, 7792.

(9) Price, S. C.; Stuart, A. C.; You, W. *Macromolecules* **2010**, *43*, 4609.

(10) Zhou, D.; Cai, N.; Long, H.; Zhang, M.; Wang, Y.; Wang, P. *J. Phys. Chem. C* **2011**, *115*, 3163.

Table 1. Optical and Electrochemical Properties of the Three Dyes

dye	λ_{max} [a]/nm ($\varepsilon/10^3$ M^{-1} cm^{-1})	E_{ox} [b]/V	E_{ox^*} [c] /V
XS32	297 (31), 355 (29), 472 (22)	0.93	−1.34
XS33	302 (38), 391 (34), 483 (39)	0.76	−1.42
XS34	300 (36), 385 (38), 502 (39)	0.82	−1.48

[a] Absorption spectra were measured in CH_2Cl_2 solutions. [b] First oxidation potentials (vs NHE) in acetonitrile internally calibrated with ferrocene (0.63 V vs NHE). [c] E_{ox^*} were estimated from Figure S4, SI.

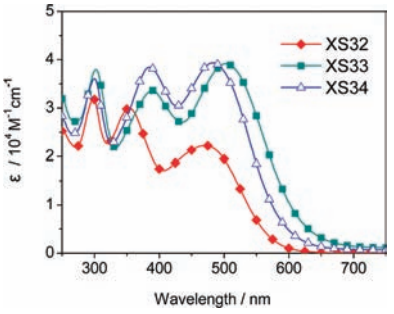

Figure 2. Absorption spectra of dyes in dichloromethane.

The three dyes exhibit two reversible oxidative waves in the cyclic voltammogram (Figure S5, SI). The first oxidation potentials of **XS33**−**34** [0.76−0.82 V vs normal hydrogen electrode (NHE)] are more negative than that of **XS32** (0.93 V vs NHE), which can be well understood on account of the electron-richness character of a BDT-based binary spacer in comparison with a single BDT unit. They are all more positive than the Nernst potential of I^-/I_3^- redox couple (0.4 V vs NHE), ensuring regeneration of the oxidized dyes by I^- after electron injection. The excited-state redox potentials of the three dyes (−1.34 to −1.48 V vs NHE) are more negative than the conduction band of TiO_2 (E_{CB}, −0.5 V vs NHE),[1b] which provide sufficient driving forces for electron injection. Thus, these oxidized dyes can be regenerated from the reduced species in the electrolyte to give an efficient charge separation.

Photovoltaic characteristics of the DSSCs based on the three dyes as well as the standard **N719** dye under AM 1.5 G condition (100 mW cm^{-2}) are displayed in Table 2, and the $J-V$ curves plotted in Figure 3. The **XS32** showed promising power efficiency of 5.68% compared to the dyes **XS33** and **XS34** featuring a binary conjugated spacer. The somewhat higher efficiency observed for **XS32** is mainly due to the relatively larger short-circuit photocurrent density (J_{SC}) and open-circuit photovoltage (V_{OC}). The best efficiency of **XS32** reached ~73% of the ruthenium dye **N719**-based standard cell fabricated and measured under similar conditions.

The preliminary evaluation of the incident monochromatic photon-to-current conversion efficiency (IPCE) of the cells based on **XS32**−**34** is displayed in Figure S6, SI. The **XS32**-sensitized cell showed absorption wavelength

Table 2. DSSCs Performance Parameters of the Three Dyes With **N719** As a Reference

dye	J_{SC}/ mA cm^{-2}	V_{OC}/mV	*ff*	η/%	τ/ms
XS32[a]	11.9	713	0.67	5.68	98
XS32[b]	6.8	620	0.67	2.82	11
XS33[a]	10.4	627	0.64	4.17	21
XS33[b]	7.3	612	0.68	3.04	9
XS34[a]	11.5	675	0.65	5.05	26
XS34[b]	7.5	636	0.68	3.24	18
N719[a]	14.6	735	0.72	7.73	

[a] Dye bath concentration of 300 μM. [b] Dye bath concentration of 30 μM.

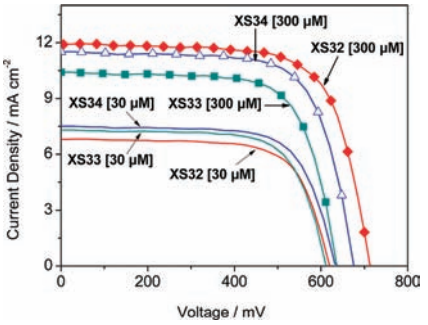

Figure 3. $J-V$ curves of DSSCs based on the three dyes. Two different dye bath concentrations (300 and 30 μM) were used for prepartion of TiO_2 electrode.

ranges from 400 to 700 nm, with a maximum of 89% at 497 nm. Solar cells based on **XS33** and **XS34** show broad IPCEs in accordance to the broad absorption spectrum achieved by increasing the π-linker conjugation. According to the absorption measurements of **XS32**−**34** on TiO_2 transparent films (Figure S2b, SI), it is found that the absorbance-to-photocurrent conversion efficiency (APCE) values around the maximum are in the order of **XS33** < **XS34** < **XS32**.

The V_{OC} values are in the sequence of **XS33** < **XS34** < **XS32**. When the binary conjugated spacer is displaced by the single spacer, the V_{OC} rises remarkably (e.g., spacer from EDOT-DBT to DBT, V_{OC} rises from 627 to 713 mV). The respectable increase of V_{OC} obtained by the delicate change in molecular structure is intriguing. To scrutinize the origin of the improvement in V_{OC}, measurement of the electrochemical impedance spectroscopy (EIS) is performed. Typical EIS Nyquist and Bode phase plots measured in the dark under forward bias (−0.7 V) are shown in Figure 4. The larger semicircle at lower frequencies represents the interfacial charge-transfer resistances (R_{CT}) at the TiO_2/dye/electrolyte interface.[12] The fitted R_{CT} increases in the order of **XS33** (92 Ω) < **XS34** (145 Ω) < **XS32** (588 Ω),

(11) Fabregat-Santiago, F.; Garcia-Belmonte, G.; Bisquert, J.; Zaban, A.; Salvador, P. *J. Phys. Chem. B* **2002**, *106*, 334.
(12) Lagemaat, J.; Park, N.; Frank, A. *J. Phys. Chem. B* **2000**, *104*, 2044.

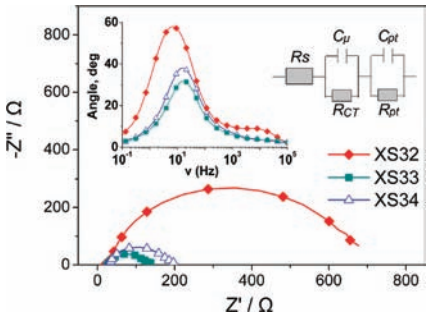

Figure 4. Nyquist plots and Bode phase plots (insert) for DSSCs based on the three dyes measured in the dark under −0.7 V bias. Top right corner is the equivalent circuit.[11]

which is consistent with the sequence of V_{OC} values in the devices. The larger R_{CT} value means that the electron recombination from the conduction band to the electrolyte occurs more difficultly. Clearly, electron recombination in devices based on **XS33** and **XS34** is faster than that of **XS32**. By fitting the EIS curves, another important parameter for DSSCs, electron lifetime (τ), could be extracted from the chemical capacitance (C_μ) and R_{CT} using $\tau = C_\mu \times R_{CT}$. The fitted τ increases in the order of **XS33** (21 ms) < **XS34** (26 ms) < **XS32** (98 ms), giving an explanation of the different V_{OC} yielded by DSSCs based on the three dyes.

Recently, several research groups have found that effective surface blocking is essential for long electron lifetime.[13] To study how surface blocking for the different dyes influences the V_{OC}, different dye bath concentrations (300 and 30 μM) were used for the preparation of TiO_2 electrode. As shown in Figure 3, the J_{SC} increases with elevated dye loading for all three dyes. Furthermore, when increasing the dye load for **XS32**-based solar cells, the V_{OC} rises remarkably from 620 to 713 mV. In contrast, the enhancements of V_{OC} for **XS33** and **XS34**-based solar cells were not obvious. It suggests that the surface blocking effect for the three dyes is on the order of **XS32** > **XS34** > **XS33**. We also derived the surface coverages (Γ) of the three dyes. It is found that the surface coverage of **XS32** (6.92×10^{-7} mol cm^{-2}) is ~1.7-fold higher than that of the other dyes (4.01×10^{-7} and 4.23×10^{-7} mol cm^{-2} for **XS33** and **XS34**, respectively). The increased dye loading of **XS32** relative to **XS33** and **XS34** significantly contributes to the observed superior surface blocking. Apart from the surface blocking, the interaction between dye and acceptor species needs to be evaluated for all new candidate dyes. In a study on the V_{OC} of DSSCs using ruthenium phthalocyanine dyes, O'Regan et al. claimed that the presence of sensitizing dyes promoted electron recombination from the FTO electrode to the redox electrolyte because of complex formation between dyes and I_3^- (or I_2).[14] We have performed similar forward bias current density measurements by adding the three dyes to the redox electrolyte (Figure S7, SI). It is found that the recombination reaction as the oxidation onset increases in the sequence of **XS33** < **XS34** < **XS32**, which is consistent with the trend observed for V_{OC}. It is possible that **XS33** and **XS34** with more conjugated dye structures increase the concentration of I_3^- at the TiO_2 surface. These results give an explanation of the different electron lifetimes yielded by DSSCs based on the three dyes.

To get further insight into the molecular structure and electron distribution of dyes, the geometries of the dyes are optimized by density functional theory (DFT) calculations at the B3LYP/6-31G(d) level (Figures S11 and S12, SI). The highest occupied and lowest unoccupied molecular orbitals (HOMOs and LUMOs, respectively) in the dyes largely populate on the triphenylamine moiety and anchoring carboxylic group, respectively. Thus, the HOMO−LUMO excitation induced by light irradiation could move the electron distribution from the triphenylamine part to the cyanoacrylic acid segment. Preliminary temperature-dependent DFT (TDDFT) computations (Table S1, SI) also highlight the electron-donating character of BDT toward excitation. There are two electronic transitions (HOMO-1→LUMO and HOMO-2→LUMO) contributing to the uninterrupted strong absorption between 350 and 550 nm for the dyes. Both the transitions have significant oscillator strength (f) and extent of charge transfer from the BDT to the 2-cyanoacrylic acid, revealing the advantages of DBT units in ameliorating the spectral response of the triphenylamine dyes.

In summary, we developed new benzo[1,2-*b*:4,5-*b*′]-dithiophene-containing organic dyes with single or binary π-conjugated spacers. These dyes exhibit intense and broad electronic absorption. The fabricated DSSCs from **XS32** exhibit high efficiencies reaching ~73% of the standard cell using **N719** as the sensitizer. The results demonstrate that BDT unit can produce high V_{OC} in DSSCs and is a promising candidate for the effective sensitizer. Further applications of the BDT derivatives to the organic dyes are now in progress, and we believe that improvement of efficiency can be achieved by careful molecular design.

Acknowledgment. We gratefully acknowledge the financial support from the National 863 Program (2009AA-05Z421), the National Natural Science Foundation of China (21003096), and the Tianjin Natural Science Foundation (09JCZDJC24400).

Supporting Information Available. Synthetic procedures and characterization for new compounds, absorption and emission spectra, cyclic voltammogram, IPCEs action spectra, plots of R_{CT}, C_μ, and τ, frontier molecular orbitals of the dyes and TDDFT calculation. This material is available free of charge via the Internet at http://pubs.acs.org.

(13) (a) Miyashita, M.; Sunahara, K.; Nishikawa, T.; Uemura, Y.; Koumura, N.; Hara, K.; Mori, A.; Abe, T.; Suzuki, E.; Mori, S. J. *J. Am. Chem. Soc.* **2008**, *130*, 17874. (b) Marinado, T.; Nonomura, K.; Nissfolk, J.; Karlsson, M. K.; Hagberg, D. P.; Sun, L.; Mori, S.; Hagfeldt, A. *Langmuir* **2010**, *26*, 2592. (c) Ning, Z. J.; Zhang, Q.; Pei, H. C.; Luan, J. F.; Lu, C. G.; Cui, Y. P.; Tian, H. *J. Phys. Chem. C* **2009**, *113*, 10307. (d) Lu, M.; Liang, M.; Han, H.; Sun, Z.; Xue, S. *J. Phys. Chem. C* **2011**, *115*, 274. (e) Liang, M.; Lu, M.; Wang, Q.; Chen, W.; Han, H.; Sun, Z.; Xue, S. *J. Power Sources* **2011**, *196*, 1657. (f) Ning, Z.; Fu, Y.; Tian, H. *Energy Environ. Sci.* **2010**, *3*, 1170.

(14) O'Regan, B. C.; López-Duarte, I.; Martínez-Díaz, M. V.; Forneli, A.; Albero, J.; Morandeira, A.; Palomares, E.; Torres, T.; Durrant, J. R. *J. Am. Chem. Soc.* **2008**, *130*, 2906.